LBL-30900
Preprint

Lawrence Berkeley Laboratory
UNIVERSITY OF CALIFORNIA

Materials & Chemical Sciences Division

Submitted to Physical Review Letters

The Dynamics of Electronically Inelastic Collisions from 3-Dimensional Doppler Measurements

A.G. Suits, P. de Pujo, O. Sublemontier, J.-P. Visticot,
J. Berlande, J. Cuvellier, T. Gustavsson,
J.-M. Mestdagh, P. Meynadier, and Y.T. Lee

June 1991

Prepared for the U.S. Department of Energy under Contract Number DE-AC03-76SF00098

DISCLAIMER

LBL-30900

THE DYNAMICS OF ELECTRONICALLY INELASTIC COLLISIONS FROM 3-DIMENSIONAL DOPPLER MEASUREMENTS

A. G. Suits, P. de Pujo, O. Sublemontier, J.-P. Visticot
J. Berlande, J. Cuvellier, T. Gustavsson,
J.-M Mestdagh, and P. Meynadier
DRECAM/SPAM
CEN Saclay
91191 Gif-sur-Yvette Cedex, France

Y. T. Lee
Department of Chemistry
University of California
and
Chemical Sciences Division
Lawrence Berkeley Laboratory
Berkeley, CA 94720 USA

June 1991

This work was supported by the Director, Office of Energy Research, Office of Basic Energy Sciences, Chemical Sciences Division, of the U.S. Department of Energy under Contract No. DE-AC03-76SF00098.

The Dynamics of Electronically Inelastic Collisions From 3-Dimensional Doppler Measurements

A. G. Suits*, P. de Pujo, O. Sublemontier, J.-P. Visticot, J. Berlande, J. Cuvellier, T. Gustavsson†, J.-M. Mestdagh, and P. Meynadier
DRECAM/SPAM
CEN Saclay
91191 Gif-sur-Yvette Cedex, France

and

Y. T. Lee
Chemical Sciences Division
Lawrence Berkeley Laboratory and
Department of Chemistry
University of California
Berkeley CA 94720

Abstract

Flux-velocity contour maps were obtained for the inelastic collision process $Ba(^1P_1) + O_2,N_2 \rightarrow Ba(^3P_2) + O_2, N_2$ from Doppler scans of scattered $Ba(^3P_2)$ taken over a range of probe laser directions in a crossed beams experiment. Collision with O_2 resulted in sharply forward scattered $Ba(^3P_2)$, with efficient conversion of inital electronic energy into O_2 internal energy and little momentum transfer. Collision with N_2 was dominated by wide-angle scattering with most of the available electronic energy appearing in product translation. The results suggest the importance of large impact parameter collisions and a near-resonant energy transfer in the case of O_2, while for N_2 close collisions dominate despite the presence of an analogous near-resonant channel. The results represent the first direct experimental demonstration of a near-resonant quenching process.

PACS numbers: 34.50.Lf, 34.50.Rk
*Present address: *Department of Chemistry, University of California, Berkeley, CA 94720*
†Present address: *DRECAM/SCM/URA 331 CNRS, CEN/Saclay 91191 Gif-sur-Yvette Cedex, France.*

Quenching collisions between molecules and electronically excited atoms are non-adiabatic processes of central importance in laser physics and atmospheric and combustion chemistry. Despite this, experimental progress in understanding the dynamics of these collisions has been slow owing to the fact that the number of possible final states may be quite large and interference from ground state processes can be overwhelming. Quenching of $Na(3^2P)$ has been studied in some detail in crossed beams experiments involving a variety of molecular collison partners, and considerable insight has been obtained into the broad features of these processes.[1-5] Yet the difficulty in obtaining differential cross sections and the problems posed by near-resonant processes for conventional detection methods have hampered the full exploitation of the power of crossed beams techniques in the study of these collisions. Following pioneering experiments of Kinsey and coworkers[6], Doppler spectroscopy has proved to be a versatile tool in the study of atom-atom collisions[7], photodissociation[8], and even reactive scattering[10,11] and offers a means of circumventing background problems inherent in the study of inelastic collisions. But the application of Doppler techniques has generally been limited to situations in which only one final state is involved and the final translational energies are known by virtue of the state probed. In that case since the scattered species is confined to the surface of a sphere, the Doppler scan along the relative velocity vector can reveal the differential cross sections directly.[6] For the case in which numerous final states are involved and a range of product translational energies exist, no such simple relation holds: a range of

center-of-mass velocities and angles may simultaneously satisfy the Doppler resonance condition.[10,11] We have successfully carried out investigation of such a case by taking Doppler scans over a range of probe laser angles and applying the "forward convolution" technique widely used in crossed beam studies of reactive scattering[12,13] to derive angular and translational energy distributions for systems in which the final translational energies are not known. We applied these methods to obtain complete contour maps of $Ba(^3P_2)$ flux from the inelastic processes $Ba(^1P_1) + O_2,N_2 \rightarrow Ba(^3P_2) + O_2,N_2 + 0.564$ eV. The contour map reveals near-resonant production of $Ba(^3P_2)$ in $Ba(^1P_1)$-O_2 collisions. In contrast, the contour map obtained for $Ba(^1P_1)$-N_2 collisions indicates that in this case this process largely remains vibrationally adiabatic, although a near-resonant contribution is seen as a minor channel.

The experimental apparatus[14] features an effusive barium atomic beam crossed at 90° by a supersonic molecular beam under single collision conditions. The 554 nm $Ba(^1S_0$-$^1P_1)$ transition was pumped by a cw single frequency ring dye laser directed through an optic fiber, perpendicular to the collision plane, to the interaction region. Doppler scans of the collisionally populated $Ba(^3P_2)$ state were made by probing the $Ba(^3P_2 \rightarrow {}^3S_1)$ transition at 790 nm while monitoring the $Ba(^3S_1 \rightarrow {}^3P_1)$ fluorescence at 739 nm. The probe laser was introduced through the same optic fiber as the pump laser for perpendicular scans, or through a second optic fiber in the collision plane for other probe laser angles. The second fiber could be rotated around the interaction region, allowing for Doppler scans from

18° to 50° from the molecular beam as illustrated schematically in Figure 1. The Doppler spectra were simulated using a computer program[7,13] in which assumed forms of the translational energy and angular distributions were used to simulate the contribution to the Doppler signal at a given laser angle and frequency offset. The result was then convoluted over the measured beam velocity distributions and a 50 MHz Lorentzian to account for power broadening. The translational energy and center of mass angular distributions were varied to obtain the best fit to the experimental results. Independent translational energy and angular distributions were assumed for each final vibrational state of the molecular collision partner, with the contributions summed to give the simulated spectra. Although the data could be fit with a single separable angular and translational energy distribution, the result was clearly artificial: the final vibrational states were thus fit separately in order to obtain physically reasonable distributions.

Results for collision with N_2 at 0.21 eV are shown in Figure 2 along with the simulated spectra. The width of the peak in the perpendicular scan (Figure 2a) indicates substantial wide angle scattering. However, the velocity component of this distribution along the relative velocity vector cannot be determined unless the probe laser direction contains a component parallel to the relative velocity vector. The scan parallel to the relative velocity vector (Figure 2b) reveals that the $Ba(^3P_2)$ distribution is generally forward scattered with respect to the barium beam. Additional scans 35° and 50° from the N_2 beam are necessary to provide the redundant information from which final fits may be obtained. These fits were

found to be very sensitive to the angular distributions but, owing to the spread in the Ba beam velocity, less so to the energy distributions. The simulations then allow quantitative interpretation of these observations, summarized in the flux-velocity contour map shown in Figure 3. Important contributions come from all possible final N_2 vibrational states. A sharp near-resonant v=2 peak is observed near the tip of the barium beam velocity vector. Both for N_2 and O_2 there exist near-resonant final vibrational states:

$$Ba(^1P_1) + O_2(v=0) \rightarrow Ba(^3P_2) + O_2(v=3) \quad \Delta E = 6.3 \text{ meV}$$

$$Ba(^1P_1) + N_2(v=0) \rightarrow Ba(^3P_2) + N_2(v=2) \quad \Delta E = 10.6 \text{ meV}$$

This near-resonant contribution can be seen in the raw data as the sharp spike in the center of the perpendicular scan (Figure 2a). The near resonant contribution in the case of N_2 actually represents only a small fraction of the $Ba(^3P_2)$ flux when integrated over the entire scattering volume. The final fit consists of 80% v=0, 15% v=1 and 5% v=2. The simulations are quite sensitive to the contribution of the near-resonant v=2 channel. Clearly most of the $Ba(^3P_2)$ flux is forward-sideways scattered with substantial translational energy. The contour map suggests that for N_2, close collisions dominate this process. Most of the distribution falls outside the limit for v=1 excitation: the production of the ground vibrational state of N_2 is strongly favored. N_2 (v=0) rotational excitation inferred from the contour map peaks at 0.1-0.15 eV, corresponding to j=20-25. This is consistent with the significant rotational excitation anticipated from a close collision.

Some insight may be gained by comparison with the dynamics of related atom-atom collisions. Thermal energy collision of $Ba(^1P_1)$ with rare gases (RG) results in exclusive production of $Ba(^3P_2)$, and this was ascribed to inefficient or inaccessible crossings of the weakly attractive $Ba(^1P_1)$-RG ($^1\Pi$) and repulsive $Ba(^3P_{1,0})$-RG ($^3\Pi_{1,0}$) potential energy curves.[15] Crossed beam studies of the energy dependence of the cross section for $Ba(^3P_1)$ production in $Ba(^1P_1)$-Ar collisions have recently confirmed the existence of a barrier for this channel, a consequence of the location of the crossing on the repulsive wall of the $Ba(^1P_1)$-RG ($^1\Pi$) curve.[16] In the case of $Ba(^1P_1)$-N_2 collisions, the analogous repulsive triplet curve is now a set of three repulsive triplet surfaces, each corresponding to a given N_2 vibrational state. On approach, the first encountered crossing seam is with the $Ba(^3P_2)$-N_2(v=2) surface, which occurs at fairly large Ba-N_2 distance. The Franck-Condon factors for this transition are likely to be unfavorable and this is consistent with the small fraction of scattered $Ba(^3P_2)$ flux we observe (5%) which originates from this crossing. Furthermore, this crossing occurs in a relatively flat region of the repulsive surface, so little deflection is likely to result for these collisions. Again this is consistent with the sharply forward scattered, near-resonant $Ba(^3P_2)$ which we observe corresponding to N_2 (v=2). The next encountered crossing will be with the N_2 (v=1) surface, with perhaps more favorable Franck-Condon factors and substantially stronger deflection. The final crossing, with N_2 (v=0), occurs at close range. Much of the electronic energy may be released into translation through the long descent on this steeply repulsive

region of the $Ba(^3P_2)$-N_2 (v=0) surface. The tendency to sideways scattering and large translational energy release thus reflects the strong coupling at this inner crossing. This is in effect an atomic picture of the collision mechanism, in which the molecular nature of N_2 is incorporated simply by its vibrational structure. But the molecular nature of N_2 is manifest in its electronic properties as well, in that the N_2^- compound state is much lower in energy than, for example, Ar^-.[17] This results in "prestretching" of the N_2 bond in the presence of the metal atom, as has been demonstrated for the Na-N_2 system.[4,5] Although this will have implication for the details of the potential energy surfaces, their overall shape, and the collision mechanism sketched above, remain unaffected.

The results for O_2, shown in Figure 4, represent a dramatic contrast to the N_2 results. The contour map obtained for $Ba(^1P_1)$-O_2 collision at 0.21 eV, shown in Figure 5, reveals the absence of the wide-angle scattering which dominates the N_2 result. The scattered $Ba(^3P_2)$ flux distribution is almost entirely composed of the near-resonant process: the peak is near the tip of the initial velocity vector of the barium beam. At that point all of the available electronic energy has become O_2 internal energy, and no momentum has been transferred in the collision. In addition, most of the $Ba(^3P_2)$ flux is confined to very small-angle scattering. The fit includes 80% v=3 and 20% v=2, with no contribution from v=0 or 1. Although our experiment does not directly address the distribution of internal energy between O_2 vibration and rotation, the small-angle scattering most likely implies large impact parameter collisions, hence little rotational excitation. The

O_2 final state distribution is thus dominated by low J, v=3. Again, this suggests a resonant mechanism in which most of the available electronic energy is efficiently coupled into O_2 vibration. Electron attachment to O_2 results in the formation of long-lived O_2^- compound states and concomitant stretching of the O-O bond.[17] The inelastic $Ba(^1P_1)$-O_2 collisions are thus likely to proceed via an ionic intermediate. In the O_2 case the potential curves will thus be well characterized by the multiple-curve-crossing model, in which a series of flat covalent surfaces representing the initial and final states are crossed by the strongly attractive Coulombic surfaces. The sharp forward scattering again implies a transition at long range, in a flat region of the triplet surface. This near-resonant O_2 distribution illustrates the power of the Doppler technique: the inelastic process is readily apparent despite the fact that the peak of its distribution is superimposed on the barium beam, which is many orders of magnitude more intense.

The absence of the wide-angle non-resonant $Ba(^3P_2)$ from collision of $Ba(^1P_1)$ with O_2 is quite revealing. For collision of Ba with O_2, a reactive channel yielding BaO + O exists with a large cross section and it is seen for excited state as well as ground state barium.[18] No such reaction channel is available for N_2. The low impact parameter collisions which dominate the inelastic process for N_2 apparently lead to reaction in the case of O_2, with a corresponding "hole" in the angular distribution at wide scattering angles and the absence of O_2 (v=0,1) from this process. It appears that only a limited range of impact parameters may gain

access to the crossing region while eluding the dominant reactive path in the O_2 case.

Forward convolution analysis of 3-dimensional Doppler measurements can provide insight into inelastic collision processes which are otherwise experimentally inaccessible. The results presented document a near-resonant quenching mechanism for the first time. Because the technique does not discriminate against detection of low translational energy products, it allows a complete picture of the collision process to emerge.

Acknowledgement

This work was supported by NATO Grant 99/89, and the Director, Office of Energy Research, Office of Basic Energy Sciences, Chemical Sciences Division, of the U.S. Department of Energy under Contract No. DE-AC03-76SF00098. AGS acknowledges the NSF for a graduate fellowship.

References

[1]I. V. Hertel, H. Hoffmann, and K. A. Rost, Phys. Rev. Lett., **36**, 861 (1976).

[2]I. V. Hertel, H. Hoffmann and K. A. Rost, J. Chem. Phys., **71**, 674 (1979).

[3]I. V. Hertel, Adv. Chem. Phys. **50**, 456 (1982).

[4]P. Habitz, Chem. Phys., **54**, 131 (1980).

[5]P. Achirel and P. Habitz, Chem. Phys., **78** 213 (1983).

[6]J. L. Kinsey, J. Chem. Phys., **66**, 2560 (1976).

[7]J. M. Mestdagh, P. de Pujo, J. Pascale, J. Cuvellier, and J. Berlande, Phys. Rev. A, **35**, 1043 (1987).

[8]E. F. Cromwell, D. J. Liu, M. J. J. Vrakking, A. H. Kung, and Y. T. Lee, J. Chem. Phys., **92**, 3230 (1990).

[9]B.Girard, N. Billy, G. Gouedard and J. Vigue, submitted to Europhysics Letters.

[10]E. L. Murphy, J.H. Brophy, G. S. Arnold, W. L. Dimpfl, and J. L. Kinsey, J. Chem. Phys., **70**, 5910 (1979).

[11]R. Schmiedl, H. Dugan, W. Meier and K. H. Welge, Z. Phys. A **304**, 137 (1982).

[12]E. A. Entemann, J. Chem. Phys., **55**, 4872 (1971).

[13]R. Buss, Ph. D. Thesis, Univ. of Calif., Berkeley, (1972).

[14]J. Cuvellier, J. M. Mestdagh, J. Berlande, P. de Pujo, and A. Binet, Rev. Phys. Appl. **16**, 679, (1981).

[15]W. H. Breckenridge and C. N. Merrow, J. Chem. Phys. **88**, 2329 (1988).

[16]J. P. Visticot, J. Berlande, J. Cuvellier, J.M. Mestdagh, P. Meynadier, P. de Pujo, O. Sublemontier, A. Bell and J. Frey, J. Chem. Phys. **93**, 5354 (1990).

[17]G. J. Schulz, Rev. Mod. Phys., **45**, 423 (1973).

[18]T. P. Parr, A. Freedman, R. Behrens Jr., and R. R. Herm, J. Chem. Phys., **72** 5163 (1980). J. M. Mestdagh, P. Meynadier, P. de Pujo, O. Sublemontier, J. P. Visticot, C. Alcaraz, J. Berlande, and J. Cuvellier, Chem. Phys. Lett. 164, 5 (1989).

Figure Captions

1. Schematic illustration of 3-dimensional Doppler technique. In addition to the three probe laser angles indicated, scans were also obtained with the probe laser directed into the collision plane.

2. Doppler scans of $Ba(^3P_2)$ produced from collision of $Ba(^1P_1)$ with N_2 at 0.21 eV collision energy. The points are experimentally measured, the lines are best fit simulations. A. Probe laser perpendicular to collision plane. B-D Probe laser in the collision plane at indicated angle with respect to O_2 beam.

3. Velocity space $Ba(^3P_2)$ flux contour map obtained from the fit shown in Figure 2 for collision of $Ba(^1P_1)$ with N_2. The nominal Newton diagram is shown with limit circles corresponding to maximum $Ba(^3P_2)$ recoil velocity for indicated final N_2 vibrational state. The v=2 contribution has been reduced by a factor of four.

4. Doppler scans of $Ba(^3P_2)$ produced from collision of $Ba(^1P_1)$ with O_2 at 0.21 eV collision energy. For details refer to Figure 2.

5. Velocity space $Ba(^3P_2)$ flux contour map obtained from the fit shown in Figure 3 for collision of $Ba(^1P_1)$ with O_2. The v=3 contribution has been reduced by a factor of 4.

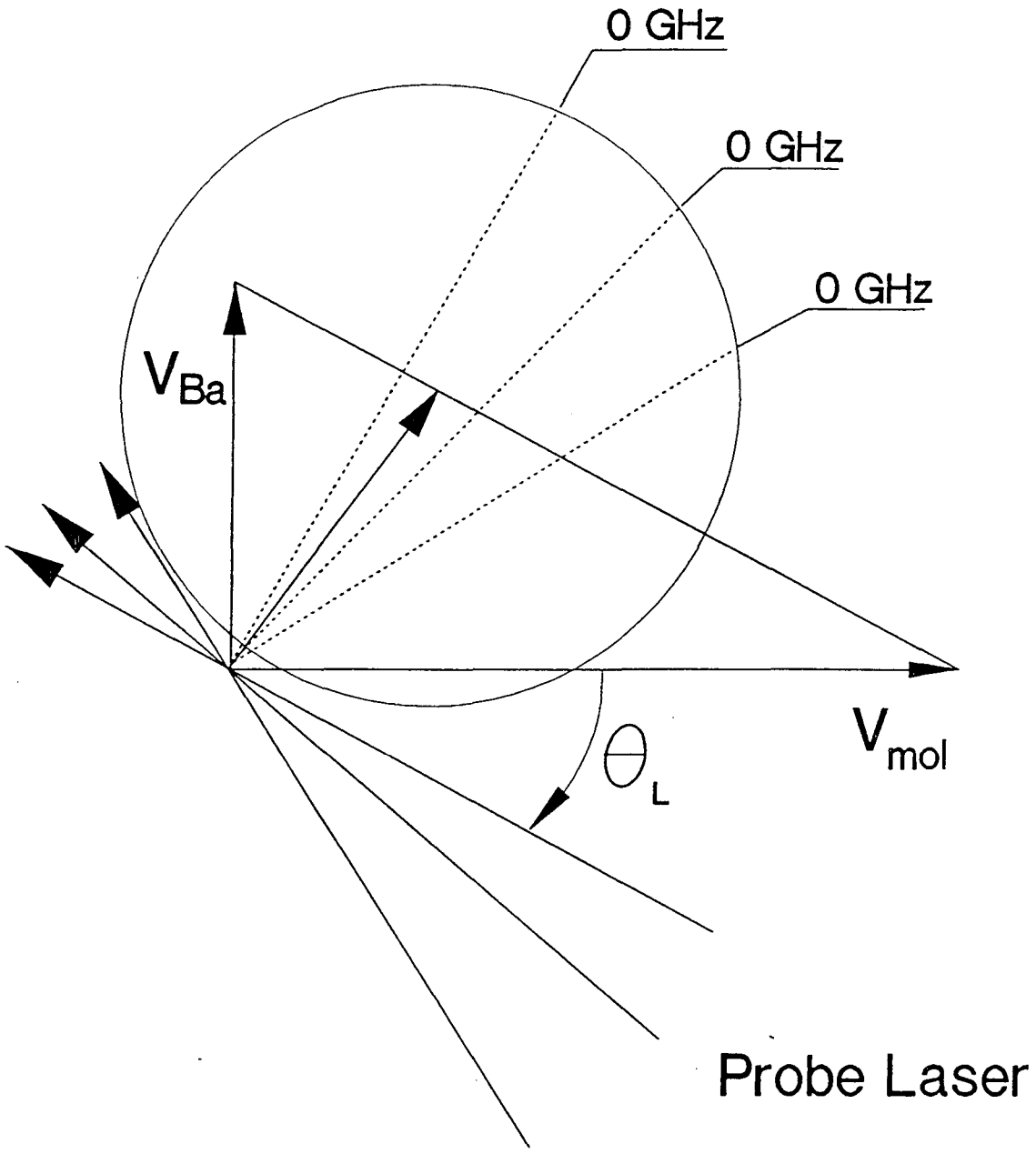

XBL 916-1187

Figure 1

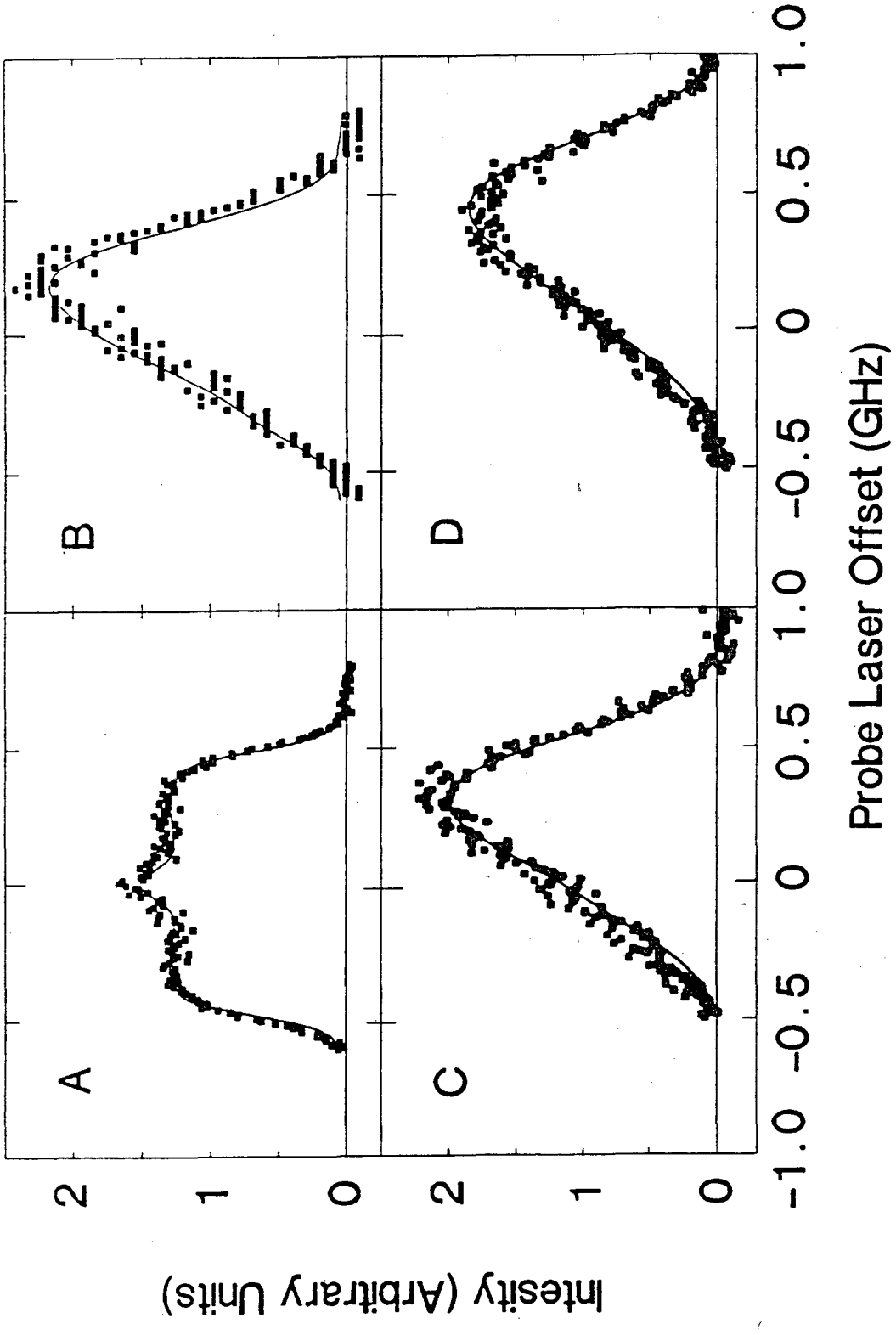

XBL 916-1188

Figure 2

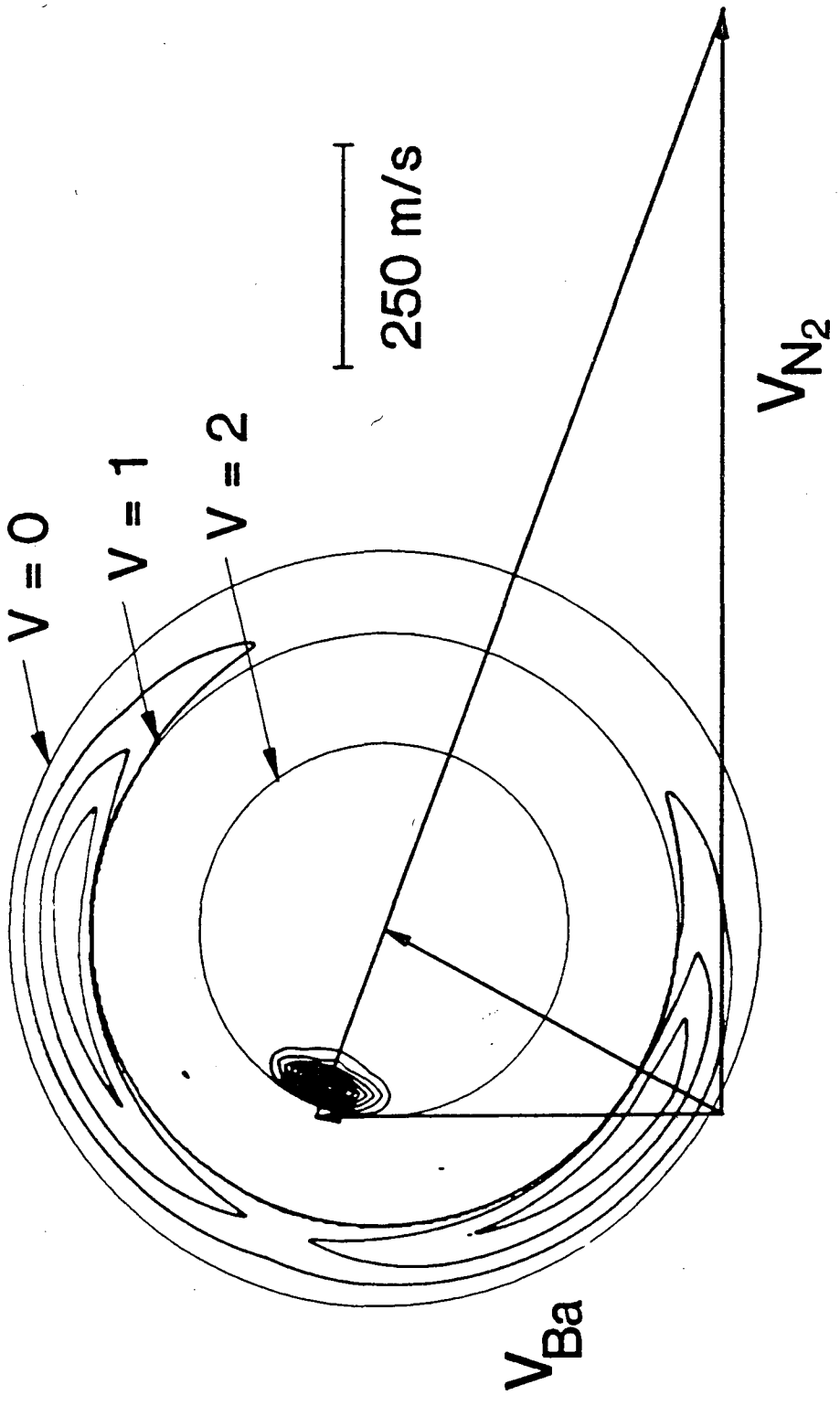

XBL 916-1189

Figure 3

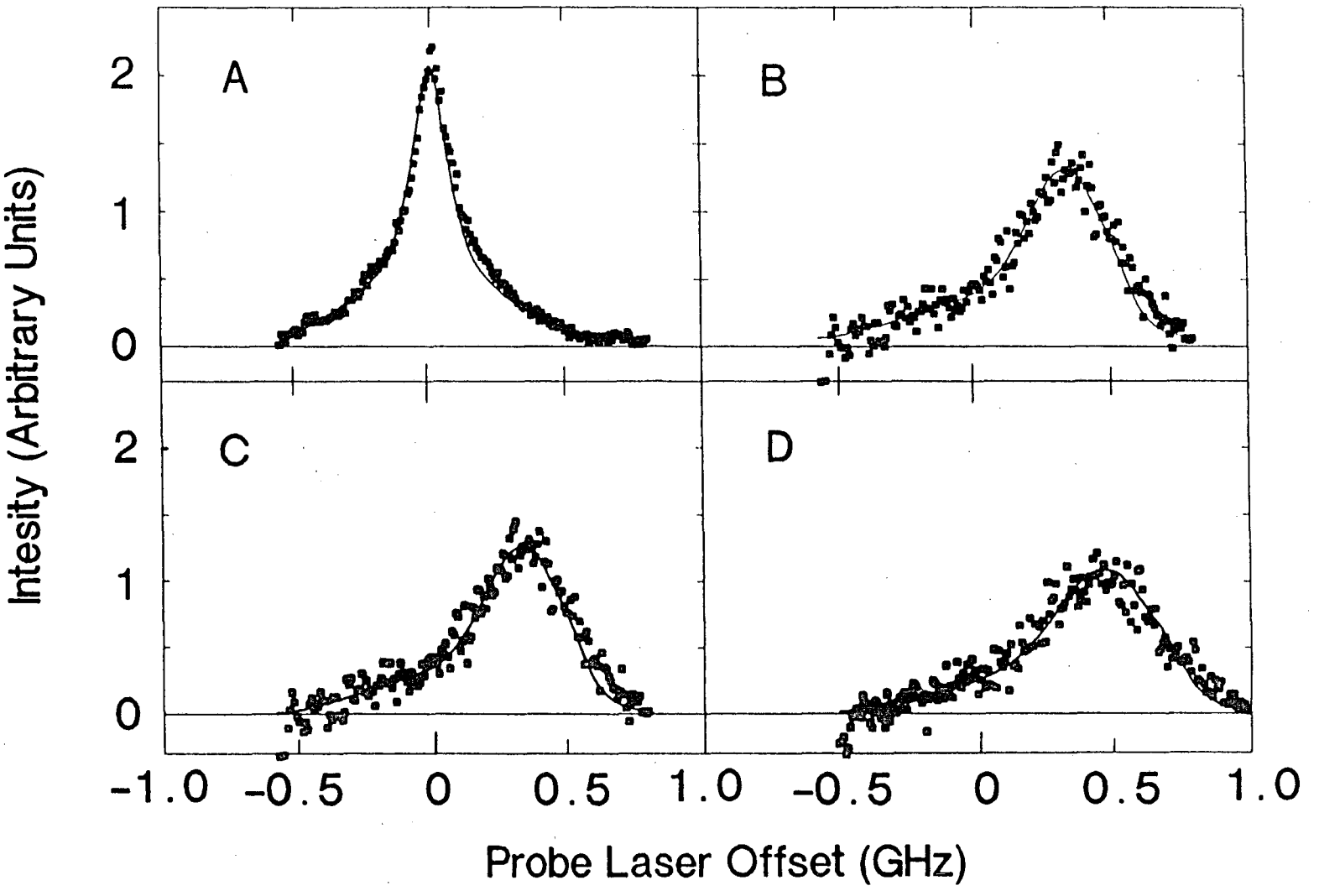

Figure 4

XBL 916-1190

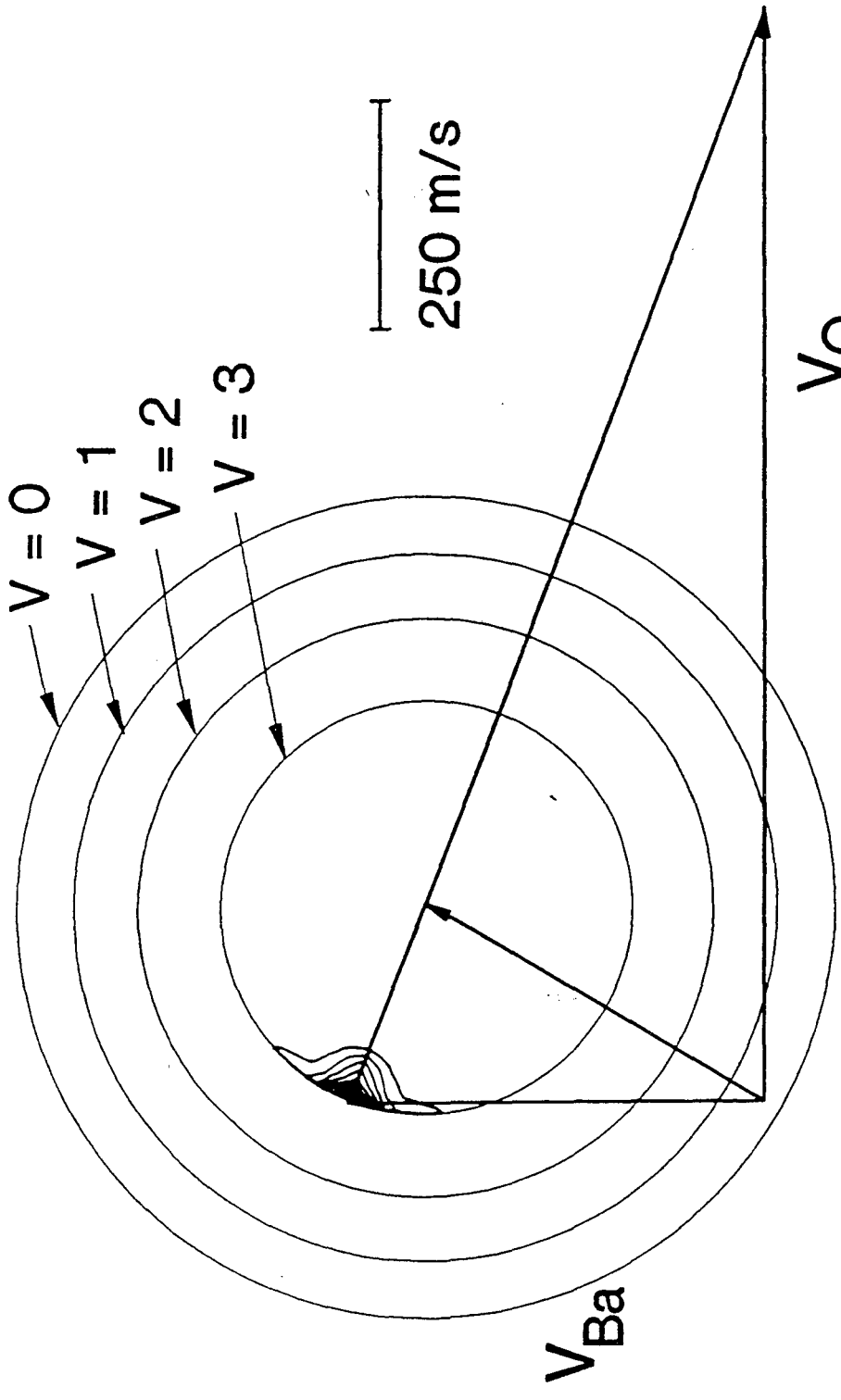

XBL 916-1191

Figure 5

LAWRENCE BERKELEY LABORATORY
UNIVERSITY OF CALIFORNIA
INFORMATION RESOURCES DEPARTMENT
BERKELEY, CALIFORNIA 94720